Monthly to annual variability of the Norwegian Atlantic slope current: connection between the northern North Atlantic and the Norwegian Sea

Øystein Skagseth

Bjerknes Centre for Climate Research, Geophysical Institute, University of Bergen, Allegaten, 70, N-5007, Bergen, Norway

Abstract

This study investigated relations between direct current measurements in the Norwegian Atlantic slope current (NwASC), the sea surface height variability from the TOPEX altimeter, and reanalysed mean sea level pressure fields. The analyses show significant coherence between the leading mslp and ssh EOF modes of variability, and again these modes are significantly coherent with variability in the NwASC for periods of a few months to 6 months. There is also some indication that similar relation is also valid for the annual scale.

The underlying physical process, inferred from the temporal evolution and spatial structure, is that variability in the westerly winds modulates the sea level slope from the northern North Atlantic into the Norwegian Sea, and thus provide a barotropic force to the Norwegian Sea. Furthermore, increased westerlies occur in phase with a steepening of the generally downward sea level slope, and this also coincides with increased NwASC. A generalized Sverdrup balance allows the observed variability in the sea level slope along the NwASC to be related to the local variability in the wind stress curl.

Author Keywords: Author Keywords: Norwegian Atlantic slope current; Sea surface height; Sea level slope; Mean sea level pressure; Wind forcing; Wind stress curl

1. Introduction

The aim of this study is to investigate the oceanic coupling between the northern North Atlantic and the Nordic Seas. This is the region of the northernmost path of the Gulf Stream with the North Atlantic current (NAC) extending into the Norwegian Sea as the Norwegian Atlantic current (NwAC). The associated fluxes of heat and salt are of major importance in modifying the regional climate. Also the relatively high salinity makes the Atlantic water (AW) a key ingredient in the transformation to dense intermediate and deep water masses as part of the global thermohaline circulation.

The basic structure of the NAC and its extension into the NwAC is known (Fig. 1). The NAC is divided into two separate northward flowing branches; along the continental slope just off the shelf break (e.g. Burrows et al., 1999; Huthnance, 1984) and one through the Iceland Basin (Perkins et al., 1998; Orvik and Niiler, 2002). A two-branch system is also observed in the Norwegian Sea: an eastern branch located just off the shelf break, hereafter denoted the Norwegian Atlantic slope current (NwASC), and a western branch farther offshore as an extension of the Iceland-Faroe frontal jet (Poulain et al., 1996; Orvik et al., 2001). Volume flux estimates of the inflowing AW (S>35.0) are about 4.5 Sv (1 Sv=10^6 m^3 s^{-1}) for the eastern branch and about 3.5 Sv for the western branch. In terms of fluxes of heat and salt the differences are somewhat larger, because the eastern branch is warmer and saltier than the western branch.

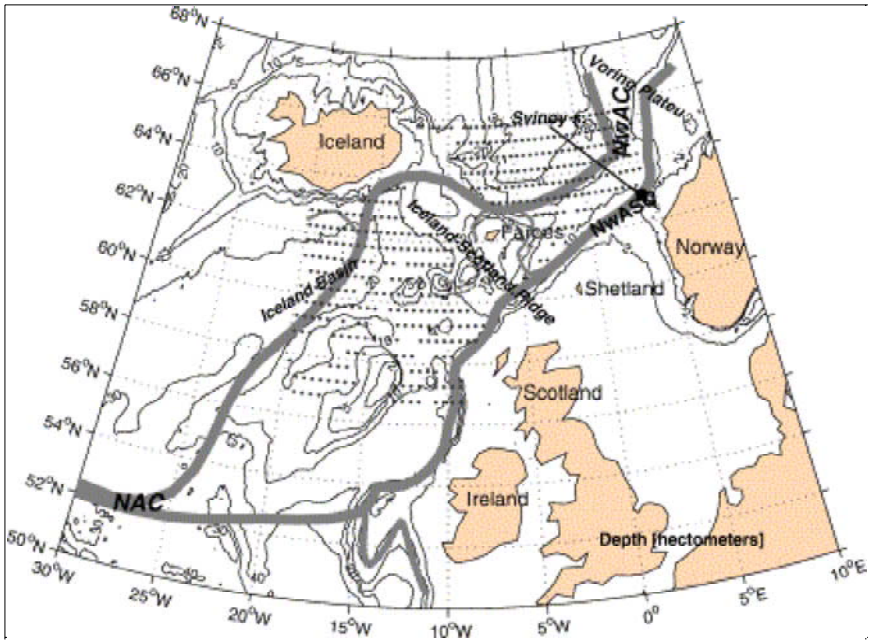

Fig. 1. Schematic of the major pathways of Atlantic water (grey lines) in the investigation area. Also included are the Svinøy section (thin black line) starting at about 62°N and going toward the north-west, the position of the moored current meter (•), and the TOPEX altimeter ssh points (•). Isobaths are contoured at 2, 5, 10, 20, 30 and 40 h.

Supposedly the eastern and western branches of the NwAC affect the climate system in the Nordic Seas and the Arctic differently. The western branch provides the interior of the Nordic Seas with more AW which again will have an impact on the regional air–sea exchanges and water mass formation, whereas the eastern branch favours fluxes into the Barents Sea and Arctic. Such arguments provide a link to the reported recent reduction of the Arctic sea ice (e.g. Johannessen et al., 1999; Rothrock et al., 1999). Thus, knowledge of the forcing controlling the relative distribution of the eastern and western branches of the NwAC is important for understanding of the climate system within the Nordic and Arctic Seas.

In contrast to the basic structure of the NAC and NwAC, which is reasonably well known, quantification of the role of the various forcing mechanisms of this northward flow is lacking. Such knowledge is essential because the type of driving mechanism may provide different constraints on the stability and the variability of the system. This is a very complex issue which certainly depends on the scale under consideration. On time scales from days to weeks, the NwASC is closely linked to the wind forcing (Skagseth and Orvik, 2002), whereas the variability of the western branch on such scales is less clear. Also, on seasonal and longer time scales the relative role of the wind and the thermohaline forcing on the variability of the NwASC is not well understood (Hansen and Østerhus, 2000; Orvik et al., 2001). However, recently Orvik and Skagseth (2003a) have suggested the averaged wind stress curl variability in the northern North Atlantic to be a forcing for inter-annual variability of the NwASC.

The focus of this study is on the eastern branch of the NwAC, the NwASC. This branch has been monitored since April 1995 by an array of current meters in the Svinøy section that runs north-westward from the Norwegian coast at 62°N and cuts through the two branches of the NwAC to the north of the Faroe-Shetland Channel (Fig. 1). Monthly to annual variabilities of the NwASC for the period from 1995 to 2000 are investigated, and causal relationships are sought in complementary data of the upstream conditions and forcing. These data are sea surface height (ssh) from the TOPEX altimeter, mean sea level pressure (mslp) and monthly climatological hydrography.

2. Observations in the NwAC

Fig. 1 outlines the large-scale surface current pattern of the Atlantic inflow, entering the Norwegian Sea mainly through two pathways—the Faroe-Shetland Channel and over the Iceland-Faroe Ridge. The western branch is an extension of the Atlantic Water running through the Iceland Basin (Perkins et al., 1998), and feeding the Iceland-Faroe Front associated with an eastward running frontal jet (Read and Pollard, 1992). It extends eastward and farther northeastward into the Norwegian Sea as the western branch of the NwAC and tends to follow the topographic slope of the Vøring Plateau (Poulain et al., 1996). The Atlantic inflow through the Faroe-Shetland Channel continues northward along the Norwegian shelf break as the NwASC. This two-branch NwAC was suggested by Poulain et al. (1996) from Lagrangian surface drifter observations. The two-fold structure with a topographically steered slope current and a frontal jet about 200–300 km farther offshore is identified in the Svinøy section by moored and shipboard observations (Orvik et al., 2001).

The hydrographic regime is characterized by the wedge-shaped warm and saline Atlantic Water overlying the fresher and colder intermediate waters (Fig. 2). Orvik et al. (2001) described the annual mean slope current as an along-isobath flow about 40 km wide. The strongest along-slope component of the current is located over the steepest slope between the 200 and 700 m isobaths with a maximum of 30 cm s^{-1} and a decrease relatively uniformly westward to zero at the 1000 m isobath. On the deeper side of the current the vertical velocity shear is in accordance with the baroclinic field (Mork and Blindheim, 2000). The tidal currents are small relative to the mean currents in this area, with the major tidal constituent M_2 of the order of 2–3 cm s^{-1} (Orvik et al., 2001).

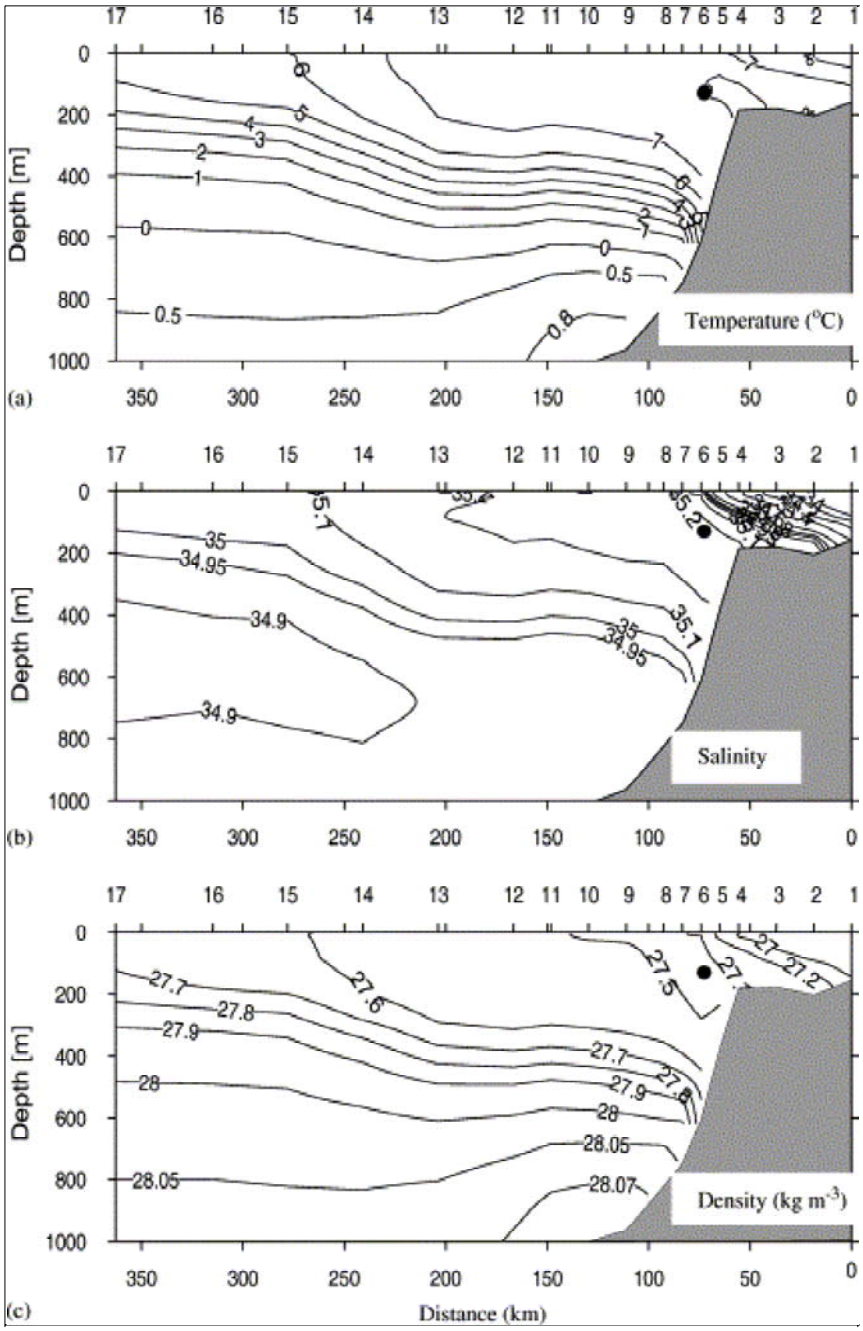

Fig. 2. Hydrography in the Svinøy section showing (a) potential temperature, (b) salinity and (c) potential density. The current meter record considered in this study was obtained over the 490 m isobath at 100 m instrument depth (•).

Orvik and Skagseth (2003b) have shown that the gross variability of the NwASC for periods longer than about 5 days can be represented by a single current meter in the core of the current. Thus, the low-frequency variability of the NwASC is presented for the period from 1995 to 2000 (Fig. 3) is based on an Aanderaa Rotating Current Meter (RCM-7) situated at 490 m water depth and instrument depth at 100 m in the core of the NwASC. The current data were originally sampled as 1 h mean values, but in Fig. 3 and elsewhere in this article, 1 month mean values of the along-slope component are used. The record suggests variability over a broad range of scales but with the seasonal cycle, winter maxima and summer minima, as the most prominent. This holds over the entire record except for the summer and fall of 1995 when the NwASC was anomalously strong relative to the subsequent summer and fall seasons. As a first crude approach seeking causal relationships for the observed variabilities of the NwASC, the NAO-index time series from Jones et al. (1997), essentially reflecting the strength of the westerlies, is also included in Fig. 3. The time series suggest that for a range of periods, from monthly to annual scale, the variabilities of the NwASC and the NAO-index tend to co-vary but the correlation coefficient (r) between the series is only 0.36. In particular, during the first

year (1995–1996) the co-variation with the NAO-index is quite different compared to the rest of the period, and the relative NwASC maximum during the summer of 1995 cannot (at least in a simple manner) be explained by the wind field. In 4 and 5 a more detailed analysis is performed to investigate the causal relationships between the variabilities in the wind forcing and the NwASC.

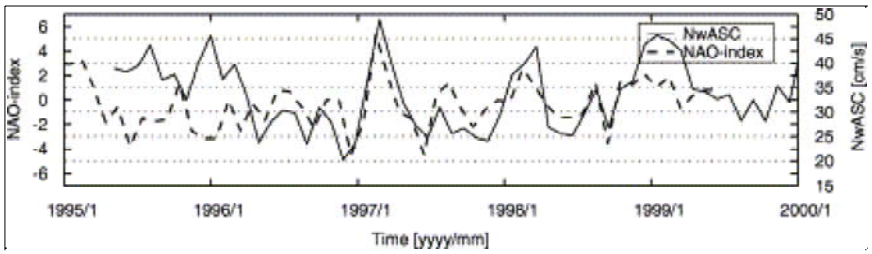

Fig. 3. Along-slope component of velocity in the NwASC based on current meters in the Svinøy section (solid line) and NAO index (dashed line). One month averaged values. The correlation coefficient (*r*) between the series is 0.36.

3. Complementary data sets

In order to evaluate the observed NwASC variabilities in a broader spatial context, data sets representing the forcing field and ocean state in the Scotland–Iceland region were analysed.

The atmospheric forcing is expressed by fields of mslp from the Norwegian Meteorological Institute. This data set was originally based on reanalysed mslp data 300 km apart interpolated to fields of 75 km×75 km spatial resolution at 6 h time intervals (Reistad and Iden, 1998). The quality of the data has been studied by Jonsson (1991), and it was found that for periods longer than about 40 h there was a good agreement between these data and the observed winds at Weather Ship M in the Norwegian Sea, at 66°N, 2°E.

Sea surface height was obtained from the TOPEX altimeter data version WOCE-PODAAC-10d-v2.0. The record covers the period from October 1992 to December 1999. The spatial resolution of the data set is 0.5°×0.5° (Fig. 1) at approximately 10 day time intervals. Corrections applied to the data include wet and dry atmospheric effects, orbit effect, tidal effects and the inverse barometer effect. Also in this data set, the mean sea level state at each grid point for the period 1993–1996 was subtracted and hence only information about the ssh variability is contained in the data. The problem of aliasing tides into longer signals, due to imperfect tidal models, was reduced by the TOPEX satellite repeat period, chosen in order to separate the periods of real oceanic phenomena from the tidal aliasing periods. The TOPEX altimeter aliasing period for the six most energetic tidal components is about 2 months (M_2, S_2, N_2, K_1 and O_1) except for P_1 where it is about 6 months (Schlax and Chelton, 1994). At these periods, special care should be taken when discussing *free* oscillations using satellite ssh data. However, since this study primarily deals with the *forced* ssh response due to wind, aliasing is not expected to be a major problem.

Monthly fields of temperature and salinity at one degree resolution and standard depths were taken from the World Ocean Atlas—1998. These data were used to estimate the annual change in the upper ocean steric height, i.e. basically the contribution upward from the main oceanic thermocline.

4. Analysis of variability

4.1. Sea surface height data

The TOPEX satellite data were analysed to investigate the ssh variability in the region of the

Iceland–Scotland Ridge. Harmonic analysis was applied to retrieve the seasonality in the data (Fig. 4). The estimated amplitudes are larger in the Norwegian Sea than in the North Atlantic, with corresponding phase varying by less than a month. Since the TOPEX data only shows variability from the mean ssh, this means that the slope of the sea surface across the Iceland–Scotland Ridge is at the maximum in March and at the minimum in September. The magnitude of this variability is of the order 10^{-7}, and thus comparable with the basin-scale meridional sea surface slope in the Atlantic Ocean. The explained variance by the ssh annual harmonic of the total ssh variance is in the range from 30–60%, with a tendency for larger values in the eastern part (toward the continental slope) of the investigation area (Fig. 4c).

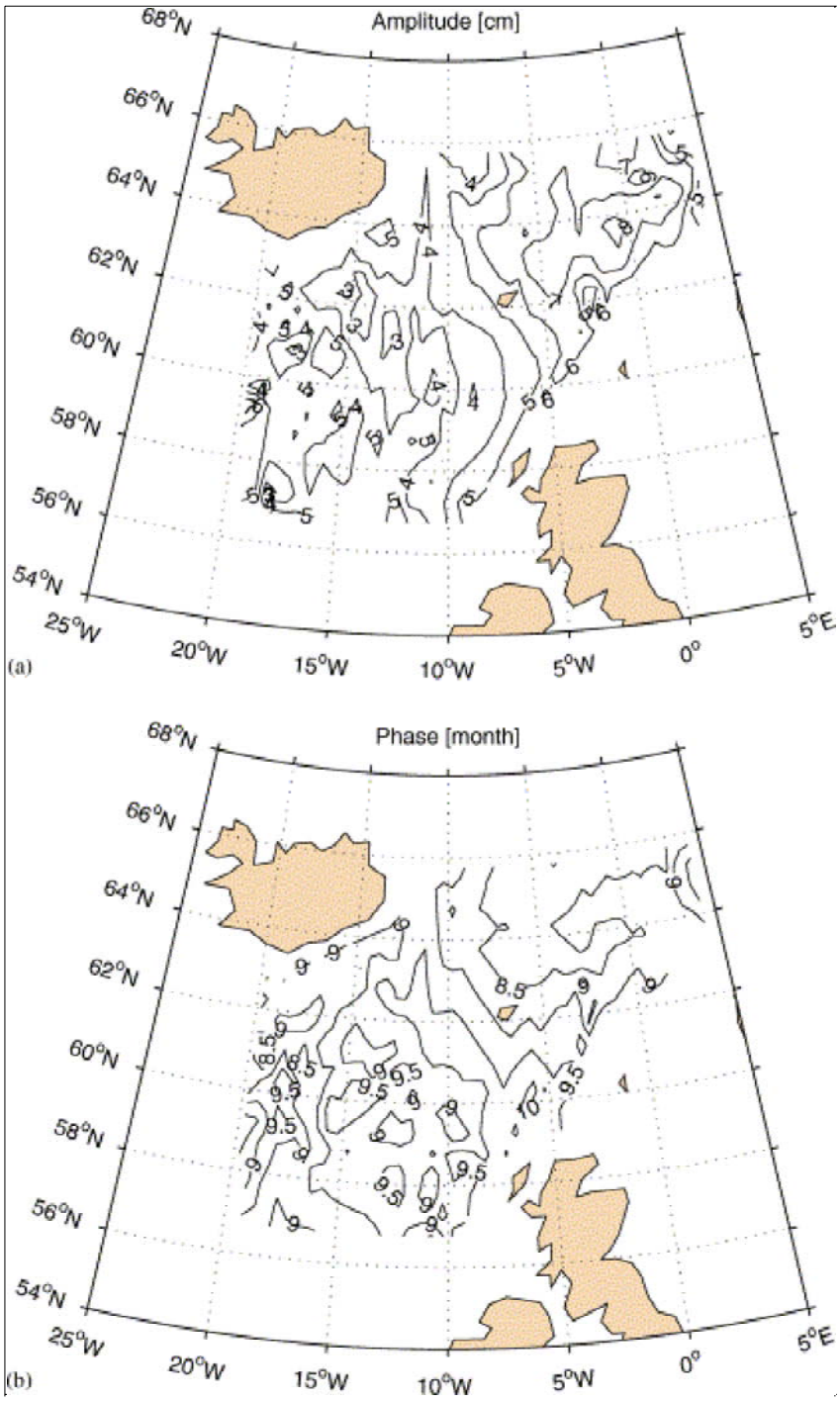

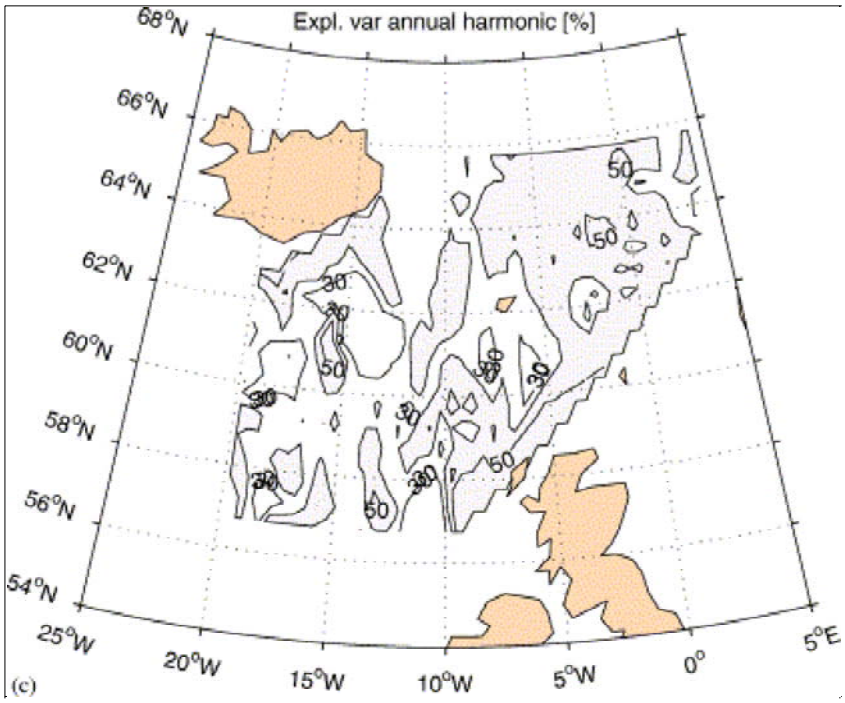

Fig. 4. Calculated sea surface height annual cycle based on the TOPEX altimeter data showing (a) amplitude in cm, (b) phase in months and (c) the amount of variance explained by the annual harmonic in percent.

The estimated annual changes in ssh due to changes in the upper ocean steric height were calculated from monthly fields of temperature and salinity from the World Ocean Atlas—1998. The annual harmonic explains about 90% of the upper ocean steric height variability for all the investigation area. The estimates are smoother, at least partly because of smoothing/interpolation of the data set onto the 1°×1° grid, but are in general of the same magnitude and phase (Fig. 5a and b) as the estimated seasonality from the TOPEX ssh data (compare with Fig. 4a and b). The largest discrepancy between these results is found in the northeastern part of the study area (about 63–64°N, 5°W–2°E) where the estimated amplitudes based on the TOPEX ssh data exceed those based on hydrography.

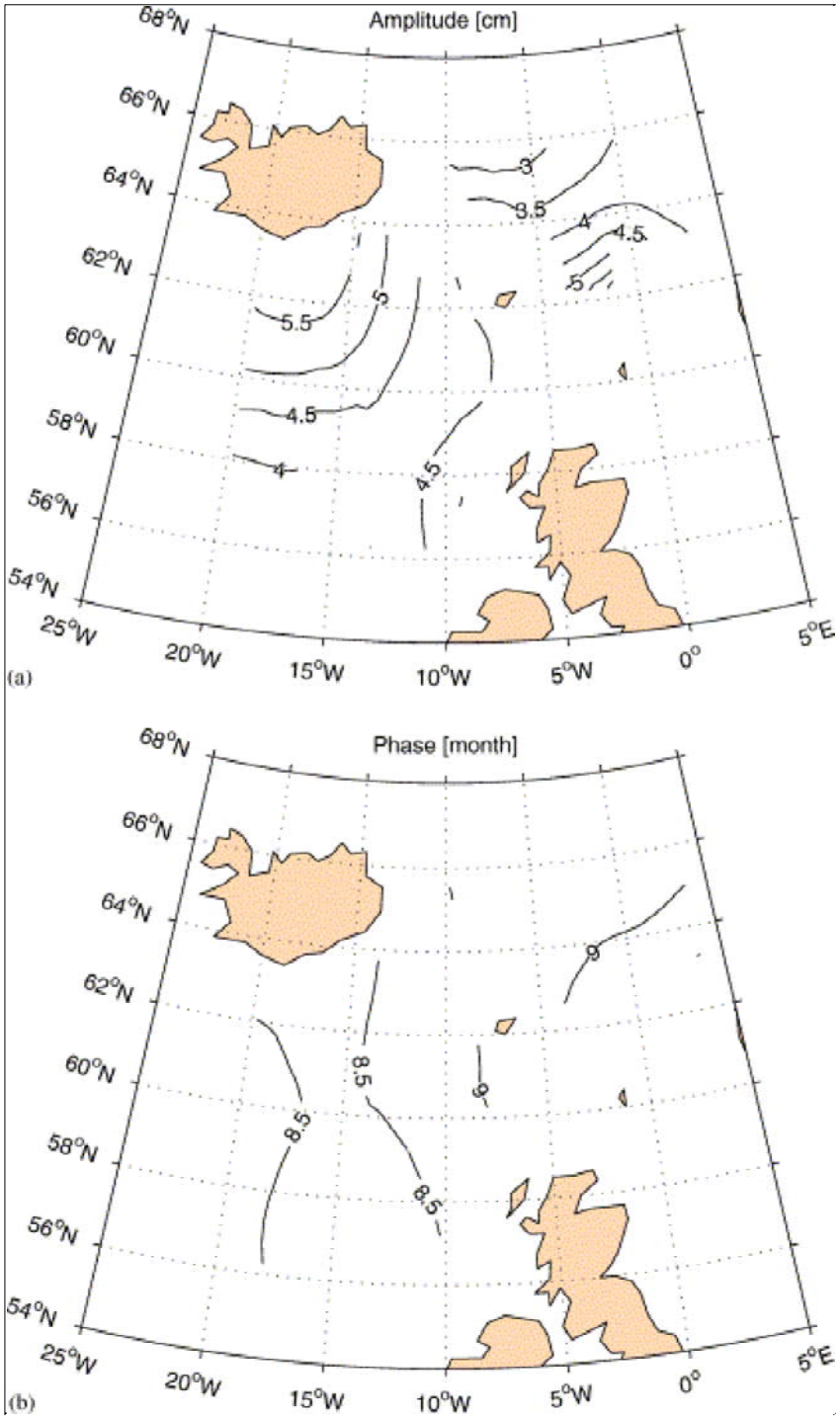

Fig. 5. Calculated steric contribution to the annual cycle sea surface height for the upper 700 m including (a) amplitude in cm and (b) phase in months. Estimates are based on the World Ocean Atlas—1998 data set.

In the appendix, the various terms contributing to variations in the ssh are discussed. Eq. (A.4) shows that steric height (η_S) is entirely due to expansion and contraction of the water column but not due to changes in mass. Changes in η_S are therefore not associated with pressure gradients and currents below a shallow surface layer. Also, because of the large-scale nature of the steric anomalies (see also Fig. 5), associated near-surface pressure gradients are generally small rendering steric height anomalies dynamically passive (Stammer, 1997). Here the focus is on the dynamically active residuals, i.e. the changes in the mass field associated with the atmospheric momentum forcing. To reveal this dynamically active signal in the observations, which is otherwise hidden, the contribution due to the annual change in upper ocean steric height (Fig. 5) was removed from the ssh data in the following analyses. This procedure has negligible effect on the results of the analyses in part 5 for periods <1 year, but becomes

important at the annual period where both the steric height contribution to the ssh and, e.g. the wind field have a profound annual period, but with a relative phase shift. This steric height correction is not perfect and thus some care should be taken when causal mechanisms at the annual period are discussed.

To further analyse the spatial and temporal variability of the ssh, an empirical orthogonal function (EOF) analysis was performed. Prior to this, the data were smoothed in time with a moving-average filter with a 1 month cut-off period. In the following, the ssh variability is discussed in terms of the leading EOF mode capturing 54.9% of the variance. This mode is both statistically significant and uniquely separated from other modes. It should be noted that the magnitudes of the explained variance depend on the size of the investigation area and the time filtering applied to the data prior to the analysis. The spatial pattern associated with this mode shows the highest magnitudes in the Norwegian Sea. The uni-pole pattern means that variabilities due to this mode are in phase in the northern North Atlantic and in the Norwegian Sea (Fig. 6a). The principal component indicates variability over a broad range of scales from months to inter-annual (Fig. 6b). Also noteworthy are two longer periodic trends through 1993–1995 and 1996–1999, separated by a "jump" in 1995. This mode includes sea surface height gradients both normal and tangential to the slope current, the NwASC in the Norwegian Sea. In a physical sense, the gradients normal to the flow can be interpreted diagnostically simply as mirroring the strength of the geostrophic flow, whereas the gradients parallel to the continental slope, i.e. in the direction of the slope current, capture variability of the barotropic forcing term in the direction of the slope current.

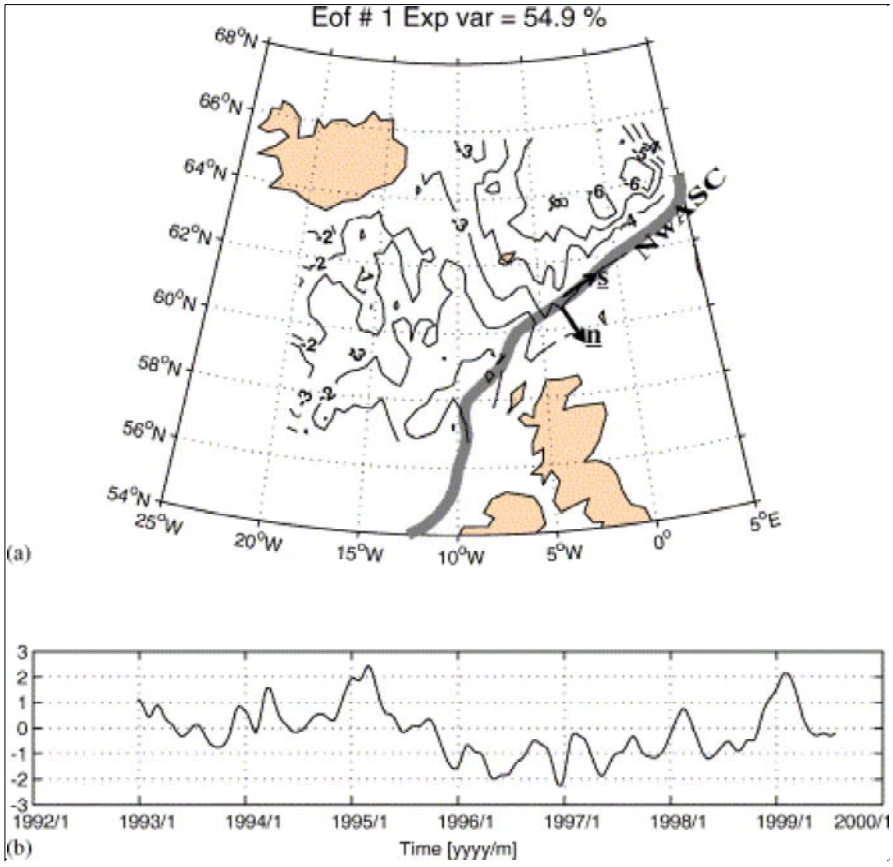

Fig. 6. EOF analysis of the TOPEX ssh data showing (a) the first EOF mode and (b) its associated principal component. Previous to plotting the EOF pattern was multiplied by the standard deviation of the principal component, and the principal component was divided by the associated standard deviation. The unit is in cm. One month low-pass filtered data. The pathway of the NwASC is included, together with the its along-stream (*s*) and cross-stream (*n*) relative direction discussed in 5 and 6.

4.2. The mean sea level pressure data

The mslp variability in the study region was retrieved by EOF analysis. Prior to the analysis the mean value at each grid point was removed and the data were smoothed in time with a moving average filter with a 1 month cut-off period in a manner similar to that used for the ssh data (Section 4.1). Here the two statistically significant EOF modes, capturing 76.5% and 12.5% of the variance, are discussed.

The leading mode contains a uni-pole pattern with centre of action just south-east of Iceland (Fig. 7a). Combined with its principal component (Fig. 7b) this mode basically represents a measure of the strength of the atmospheric lows (cyclones), and also the strength of the westerlies, with winter maxima and summer minima. Striking features are the "state-switch" in 1995–1996, and the apparent long-period trends with growing amplitudes in 1992–1995 and 1996–1999.

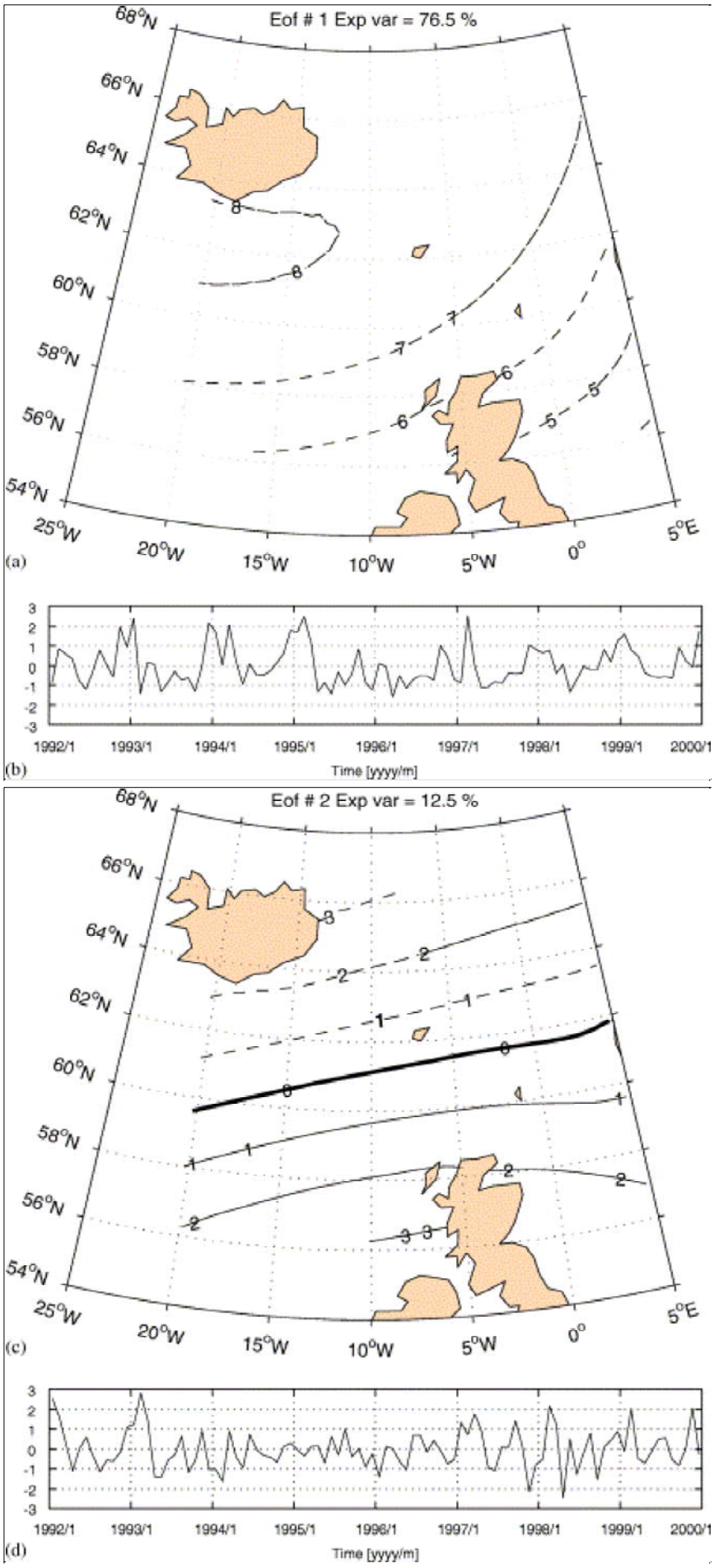

Fig. 7. EOF analysis of the Hindcast mslp data showing (a) the leading EOF mode and (b) the associated principal component, (c) the second EOF mode and (d) its associated principal component. Previous to plotting the EOF patterns were multiplied by the standard deviation of

their associated principal components, and the principal components were divided by their associated standard deviation. The unit is mbar. One month low-pass filtered data.

The second EOF mode describes a di-pole pattern that essentially modifies the strength and structure of the pattern contained in the leading EOF mode. The associated principal component shows a more pronounced high frequent variability compared to the leading mode.

5. Relations between sea surface height, the wind field and the NwASC

In this part, relations between the NwASC, the sea surface height and the wind field (mslp) are investigated on time scales from a few months to a year.

5.1. Relations between the mslp and the NwASC

Coherence analyses were performed in order to investigate relations between the strength of the NwASC and the wind field represented by the principal components associated with the leading mslp modes. The normalized time series of the NwASC together with MSLP-PC1 and MSLP-PC2 are shown in Fig. 8a and b. Coherence analysis between NwASC and MSLP-PC1 show a significant peak at the 4–6 months period and with the associated relative phase not significantly different from zero. The analysis of NwASC and MSLP-PC2 show a broad range of significant frequencies (<1/6 month) and also with the associated relative phase not significantly different from zero. Physically this means that increase/decrease in the strength of the westerly winds, as contained in the leading mslp modes, coincides with increase/decrease in the strength of the NwASC for periods up to 6 months.

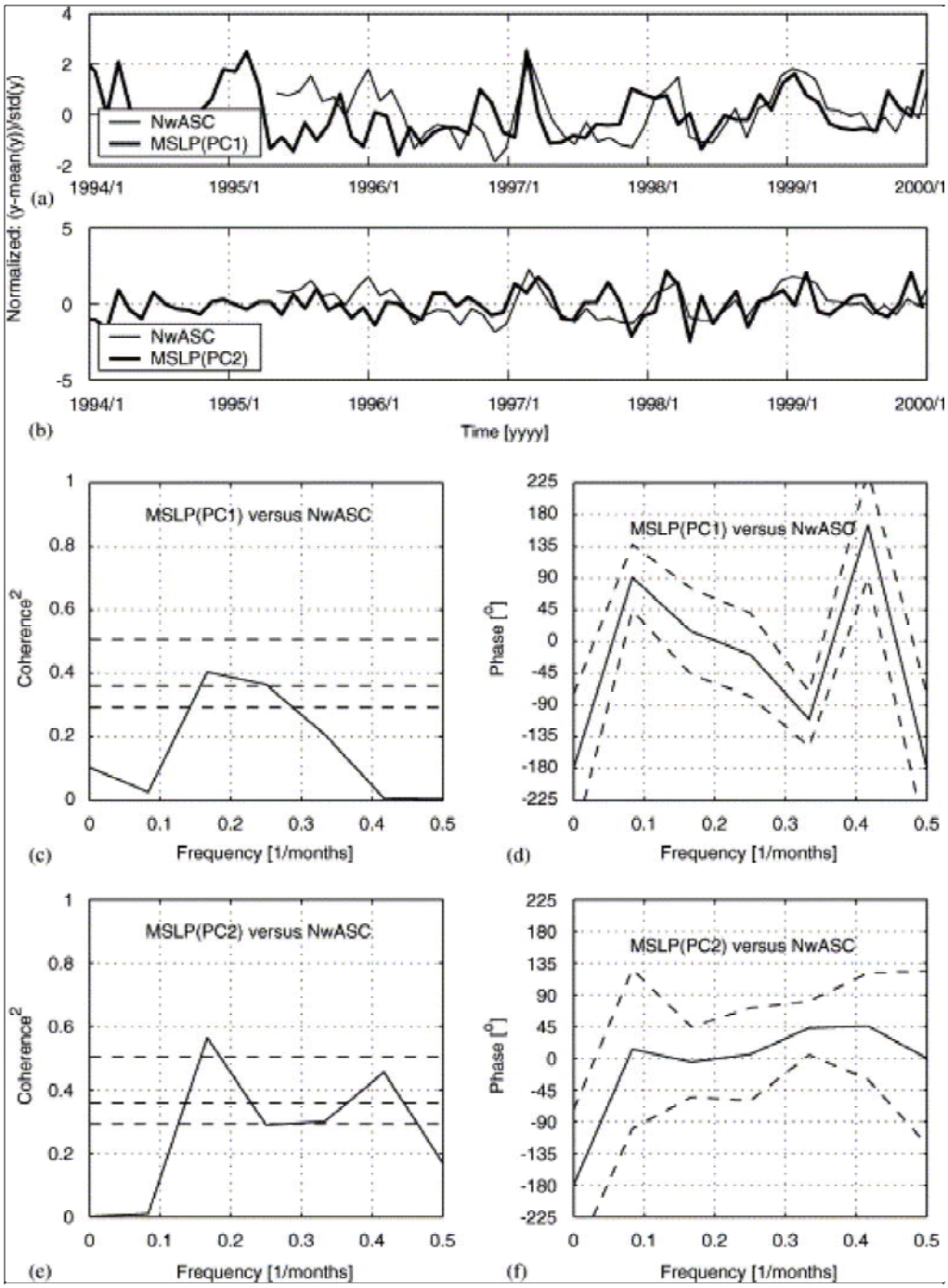

Fig. 8. Time series of the NwASC (thin line) and the principal components (thick line) of (a) the leading and (b) the second MSLP modes. Coherence analyses between the series ((c), (d)) NwASC and MSLP-PC1 and ((e), (f)) NwASC and MSLP-PC2. The lower/middle/upper horizontal dashed lines in the coherence squared estimates show the 90%/95%/99% statistical significance levels obtained from Monte Carlo analyses of 1000 synthetic series of similar length and lag-1 properties as the real series. In the phase plot, the dashed lines indicate the 95% significance interval. Positive phase means that the NwASC record trails the record of the NwASC. One month low-pass filtered data.

5.2. Relations between the mslp and the ssh

Relations between the variabilities in the sea surface height and the wind field were investigated by analysing the coherence between the principal components associated with the leading satellite ssh mode (Fig. 6) and the two leading mslp modes (Fig. 7). The normalized principal components of SSH-PC1 and MSLP-PC1 are shown in Fig. 9a. These series show a broad peak in the coherency estimates (Fig. 9c and d). For periods (*T*) >about 3 months, the coherence estimates exceed the 99% significance level. The corresponding phase between these series shows a small lag for the SSH-PC1 relative to the MSLP-PC1 but this is not

significant at the 95% level. The normalized principal components of SSH-PC1 and MSLP-PC2 are shown in Fig. 9b. These series are significantly coherent for periods of 4–6 months, and with the corresponding relative phase shift not significantly different from zero (Fig. 9e and f). The analysis shows that increase in the westerlies (variability included in the two leading mslp modes) occur in phase with the sea surface height variability as represented in leading ssh mode (Fig. 6a).

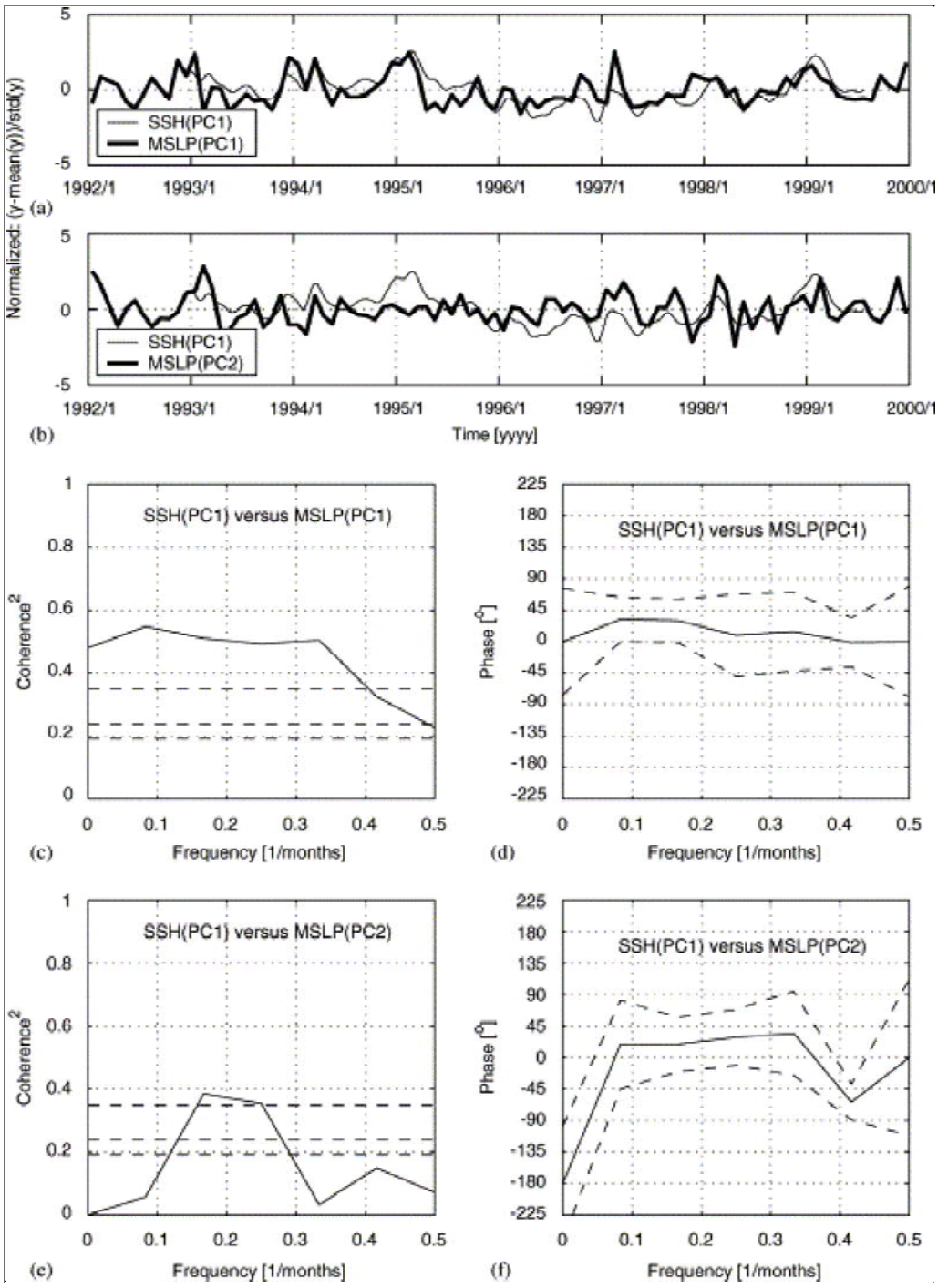

Fig. 9. Principal component time series of SSH-PC1 (thin line) and (a) MSLP-PC1 and (b) MSLP-PC2 (thick line). Coherence analysis between the series ((c), (d)) SSH-PC1 and MSLP-PC1 ((e), (f)) SSH-PC1 and MSLP-PC2. The lower/middle/upper horizontal dashed lines in the coherence squared estimates show the 90%/95%/99% statistical significance levels obtained from Monte Carlo analyses of 1000 synthetic series of similar length and lag-1 properties as the real series. In the phase plot, the dashed lines indicate the 95% significance interval. Positive phase means that the ssh record trails the record of the mslp. One month low-pass filtered data.

5.3. Relations between the ssh and the NwASC

To investigate whether relations between ssh and strength of the NwASC find support in observations a coherence analysis between the NwASC and the leading ssh mode (Fig. 6) was performed. The normalized time series of the NwASC together with SSH-PC1 are shown in Fig. 10a. The coherence analysis (Fig. 10b and c) shows statistically significant peaks for periods of 4–6 months, with phase at these periods not significantly different from zero. The physical interpretation of these results, when the spatial field associated with the leading ssh mode (Fig. 6a) is also considered, is that increased NwASC occurs in phase with increased sea level gradients both normal to the flow (mirroring a geostrophic balance) and increased negative sea level gradients in the down-stream direction of the NwASC.

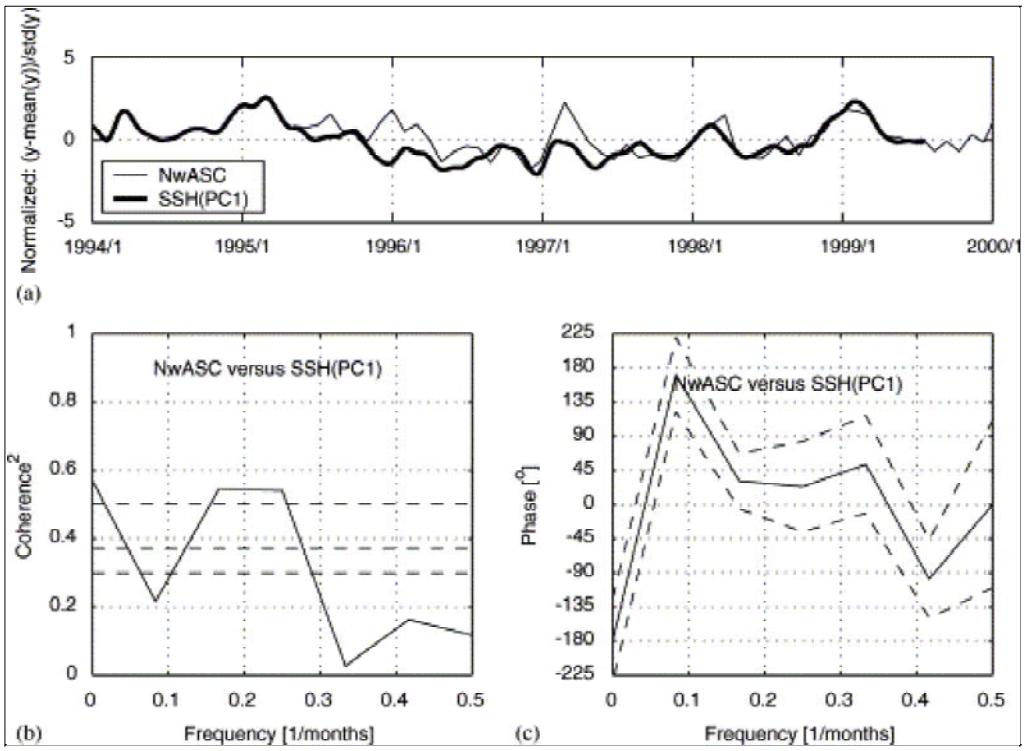

Fig. 10. Time series of the NwASC (thin line) and SSH-PC1 (thick line), and ((b), (c)) coherence analysis between the NwASC and SSH-PC1. The lower/middle/upper horizontal dashed lines in the coherence squared estimates show the 90%/95%/99% statistical significance levels obtained from Monte Carlo analyses of 1000 synthetic series of similar length and lag-1 properties as the real series. In the phase plot, the dashed lines indicate the 95% significance interval. Positive phase means that the ssh record trails the record of the NwASC. One month low-pass filtered data.

6. Discussion and concluding remarks

The analyses in the previous section show significant relations between the mslp field, the ssh field and the velocity of NwASC. The analyses show that increase in the westerlies (variability included in the two leading mslp modes) occurs in phase with both increased ssh gradients normal to the flow (mirroring a geostrophic balance) and increased negative ssh gradient along-stream the NwASC. Furthermore, this also coincides with an increase in the strength of the NwASC.

If the variabilities of the mslp, the ssh and the NwASC are linked in a physical manner and through a similar process, the analyses should result in coherency peaks at similar frequencies. Thus, there is an apparent problem with the annual period. This period is significantly coherent in the analyses between mslp and ssh, but in the analyses of mslp and current this period is not significant. However, at least partly, this discrepancy is due to the coherence analyses between ssh and mslp that considered data from January 1993, whereas the current records of the NwASC start in April 1995. The annual period appears anomalously strong during the years 1993–1995 (see Fig. 9a). When data prior to april 1995 are excluded in the coherence analysis

between mslp and ssh the coherence at the annual period is substantially reduced (relative minimum). Consequently, one cannot exclude the possibility that similar relationships between the NwASC, the mslp and the ssh also exist at the annual period.

With the statistically significant relations, it remains to discuss how these variables are linked in a physical sense. This question is of importance since we cannot exclude a priori, though it is not likely, that other forcing mechanisms cause variabilities in the NwASC and that the change in sea level is simply a response to this. A main question is how variabilities in the mslp (wind field) modulate the sea level slope along-stream the NwASC?

Enfield and Allen (1980) attempted to relate the along-slope sea level change to the surface Ekman transport assuming a compensating oppositely directed geostrophically balanced flow. However, their model does not fit the observations in this study. Instead, assuming spatial scales of hundreds of kilometres and time scales from months up to a year, an attempt is made to explain the along-slope sea level change using linearized low-frequency limit of the generalized Sverdrup relation for a barotropic flow (Willebrand et al., 1980):

$$h\bar{u}\cdot\bar{\nabla}\left(\frac{f}{h}\right)=\frac{\bar{k}\cdot\bar{\nabla}\times\bar{\tau}}{\rho h}. \quad (1)$$

where h is the depth, u is the current vector, f is the Coriolis parameter, k is the vertical unit vector, τ is the wind stress vector and ρ is the density of sea water. Sturges (1974) attempted to explain the north–south along-shore sea level slopes as being related to the latitudinal variation in the Coriolis parameter. Essentially, that would be to assume the forcing term to vanish in Eq. (1). However, in the study region the depth changes dominate relative to the change in f, the f/h and h contours tend to follow, and furthermore the wind stress curl term is significant. Assuming u to be geostrophically balanced a link between the sea level slope along the isobath (and along-stream the NwASC) and the wind stress curl is given by

$$\frac{\partial\eta}{\partial\bar{s}}=\frac{f\bar{k}\cdot\bar{\nabla}\times\bar{\tau}}{\rho g h^2\nabla(f/h)}. \quad (2)$$

where η is the sea level and s is the unit vector tangential to the isobath and thus also to the NwASC (Fig. 6a). The balance in Eq. (2) is investigated by comparing the change in sea level slope taken from the SSH-EOF1 with the local wind stress curl term (Fig. 11). The magnitude of the wind stress curl term is sensitive to the choice of h and bottom slope. However, for realistic values for these parameters, both the magnitude of these terms are of the same order and their variabilities are significantly correlated (r= 0.60). An attempt was made to estimate the sea level slope directly from the satellite ssh data, but this gave poorer correlation with the wind stress curl term. This would be in accordance with the high-frequency/small-scale noise being filtered out from the leading ssh EOF mode by the EOF decomposition. However, estimating the sea level slope from the leading ssh EOF mode is a rather crude approximation. In addition, neglected effects, e.g. the complex topography including the Iceland–Scotland Ridge, is possibly important and thus one should not expect the observations to perfectly balance the terms in Eq. (2).

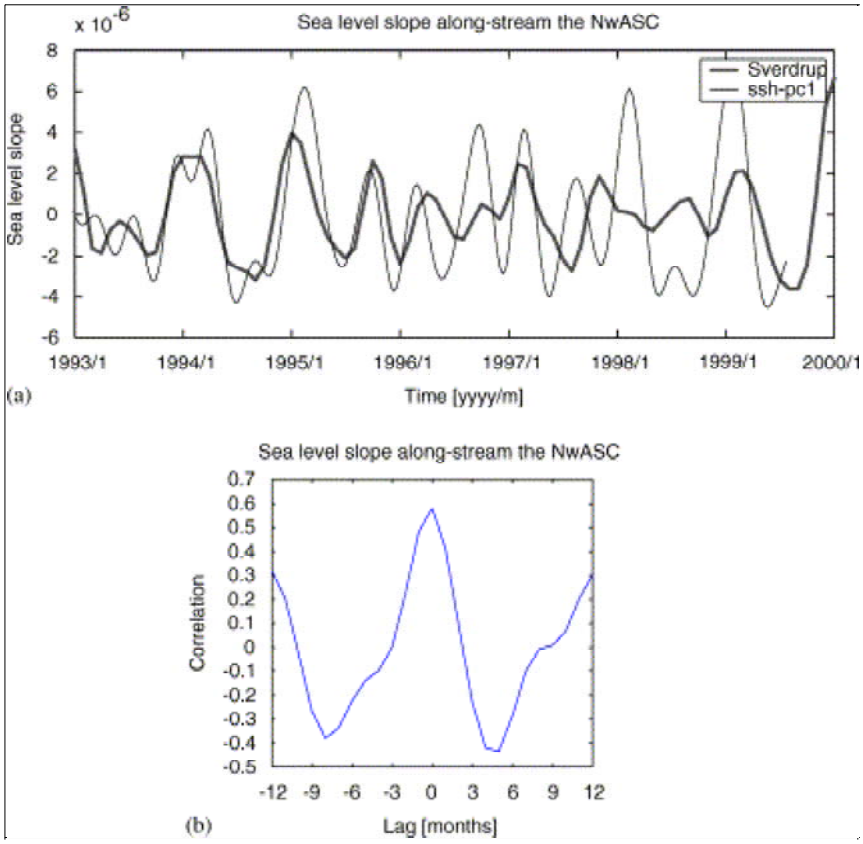

Fig. 11. (a) Time series showing variabilities of (a) the sea level slope along stream the NwASC based on the leading ssh eof mode at (59.5N, 7W) and (62N, 2E) and the variability of the wind stress curl term in Eq. (2) using the constants: f=0.7×10^{-4} s^{-1}, g=9.8 m s^{-2}, r=1027.5 kg m^{-3}, h=500 m, (f/h)=0.5×10^{-12} s^{-1}. The wind stress is taken at 61N, 2.8W about midway between sea level points. In (b) the correlation function between the series is shown with maximum correlation r=0.6 at zero lag. Based on the auto-correlation of the series the effective number of samples n=24, leading to a 99% significance level r=0.49. Prior to the analysis the series were band-pass filtered retaining periods from 3 months to 1 year.

With the indicated relationship between the wind stress curl and the sea level slope along-stream the NwASC a link to the strength of the current is needed. Some simple arguments for such a relationship can be made. Increased wind stress curl leads to increased barotropic flow toward the slope. Here, the upper (Atlantic) layer becomes thicker (see e.g. Fig. 2 or http://sam.ucsd.edu/vertical_sections/Atlantic.html) and thus transfers into a northward slope current through conservation of relative vorticity in the upper layer ($\zeta^{(u)}/H^{(u)}$=const, where $\zeta^{(u)}$ and $H^{(u)}$ are, respectively, the relative vorticity and the thickness of the upper layer). It could also be argued that an increased barotropic flow toward the continental slope would pile up water, and simply that this by geostrophic adjustment transfers into an increased slope current with the shallower depth to the right.

This study suggest the wind modulation of the sea level slope in along-stream direction as a significant forcing for variabilities of the NwASC. The data are in accordance with this mechanism being valid for time scales from a few months up to 6 months. Furthermore, the data indicate, but less clearly, that similar relations also apply to the annual cycle. This would imply that the variability of the NwASC on time scales up to and including the annual period is basically wind driven. The complex topography in the North Atlantic and Norwegian Sea region is a complicating factor, and therefore it would be valuable to investigate if the relations suggested herein are dominant balances in an ocean general circulation model run with realistic atmospheric forcing.

Acknowledgements

The author is particularly grateful to Martin Mork for initial encouragement to work along these lines. Also thanks to a number colleagues for comments on various versions of the manuscript, and to two critical but constructive anonymous reviewers. Fig. 2 was obtained from Kjell A. Mork at IMR. The TOPEX ssh data were obtained from the NASA Physical Oceanography Distributed Active Archive Center at the Jet Propulsion Laboratory, California Institute of Technology. The work has received financial support from the EU program VEINS and the NFR program NOCLIM. This is publication Nr. A39 of the Bjerknes Centre for Climate Research.

References

Burrows, M., Thorpe, S.A. and Meldrum, D.T., 1999. Dispersion over the Hebridean and Shetland shelves and slopes. *Continental Shelf Research* **19**, pp. 49–55.

Enfield, D.B. and Allen, J.S., 1980. On the structure and dynamics of monthly mean sea level anomalies along the Pacific Coast of North and South America. *Journal of Physical Oceanography* **10**, pp. 557–578.

Gill, A.E. and Niiler, P., 1973. The theory of seasonal variability in the ocean. *Deep-Sea Research* **20**, pp. 141–147.

Hansen, B. and Østerhus, S., 2000. North Atlantic–Nordic Seas exchanges. *Progress in Oceanography* **45**, pp. 109–208.

Huthnance, J.M., 1984. Slope currents and "JEBAR". *Journal of Physical Oceanography* **14**, pp. 795–810.

Johannessen, O.M., Shalina, E.V. and Miles, M.W., 1999. Satellite evidence for an arctic sea ice cover in transformation. *Science* **286**, pp. 1937–1939.

Jones, P.D., Jonsson, T. and Wheeler, D., 1997. Extension to the North Atlantic oscillation using early instrumental pressure observations from Gibraltar and South-West Iceland. *International Journal of Climatology* **17**, pp. 1433–1450.

Jonsson, S., 1991. A comparison between wind stresses, based on geostrophically derived and observed winds, at Weather Ship M in the Norwegian Sea. *Deep-Sea Research* **38**, pp. 607–615.

Mork, K.A. and Blindheim, J., 2000. Variations in the Atlantic inflow to the Nordic Seas 1955–1996. *Deep-Sea Research I* **47**, pp. 1035–1057.

Orvik, K.A. and Niiler, P., 2002. Major pathways of Atlantic water in the northern North Atlantic and Nordic Seas toward the Arctic. *Geophysical Research Letters* **29** 19, p. 1896 doi:10.1029/2002GL015002 .

Orvik, K.A. and Skagseth, Ø., 2003. The impact of the wind stress curl in the North Atlantic on the Atlantic inflow to the Norwegian Sea toward the arctic. *Geophysical Research Letters* **30** 17, p. 1884 doi:10.1029/2003GL017932 .

Orvik, K.A and Skagseth, Ø., 2003. Monitoring the Norwegian Atlantic slope current using a single moored current meter. *Continental Shelf Research* **23**, pp. 159–176.

Orvik, K.A., Skagseth, Ø. and Mork, M., 2001. Atlantic inflow to the nordic seas: current structure and volume fluxes from moored current meters, VM-ADCP and SeaSoar-CTD

observations, 1995–1999. *Deep-Sea Research I* **48**, pp. 937–957.

Perkins, H., Hopkins, T.S., Malmberg, S.A., Poulain, P.M. and Warn-Varnas, A., 1998. Oceanographic conditions east of Iceland. *Journal of Geophysical Research* **103**, pp. 21531–21542.

Poulain, P.-M., Warn-Varnas, A. and Niiler, P.P., 1996. Near-surface circulation of the Nordic Seas as measured by Lagrangian drifters. *Journal of Geophysical Research* **101** C8, pp. 18237–18258.

Read, J.F. and Pollard, R.T., 1992. Water masses in the region of the Iceland-Faeroes Front. *Journal of Physical Oceanography* **22**, pp. 1365–1378.

Reistad, M., Iden, K., 1998. Updating, correction and evaluation of the hindcast data base of air pressure, wind and waves for the North Sea, The Norwegian Sea and the Barents Sea. Research Report No. 9, The Norwegian Meteorological Institute, 42pp.

Rothrock, D.A., Yu, Y. and Maykut, G.A., 1999. Thinning of the Arctic sea ice cover. *Geophysical Research Letters* **26**, pp. 3469–3472.

Schlax, M.G. and Chelton, D.B., 1994. Aliased tidal errors in TOPEX/POSEIDON sea surface height data. *Journal of Geophysical Research* **99** C12, pp. 24761–24775.

Skagseth, Ø. and Orvik, K.A., 2002. Identifying fluctuations in the Norwegian Atlantic Slope Current by means of Empirical Orthogonal Functions. *Continental Shelf Research* **22**, pp. 547–563.

Stammer, D., 1997. Steric and wind-induced changes in TOPEX/POSEIDON large-scale sea surface topography observations. *Journal of Geophysical Research* **102** C9, pp. 20987–21009.

Sturges, W., 1974. Sea level slope along continental boundaries. *Journal of Geophysical Research* **79** 6, pp. 825–830.

Willebrand, J., Philander, S.G.H. and Pacanowski, R.C., 1980. The oceanic response to large-scale atmospheric disturbances. *Journal of Physical Oceanography* **10**, pp. 411–429.

Yan, X.H., Niiler, P.P., Nadiga, S.K., Stewart, R.H. and Cayan, D.R., 1995. Seasonal heat storage in the North Pacific: 1976–1989. *Journal of Geophysical Research* **100**, pp. 6899–6926.

Appendix. Theory

Following Stammer (1997) and discussed in detail by Gill and Niiler (1973) the SSH, η, (corrected for the inverse barometer effect), can be expressed by the sum of three terms

$$\eta = \eta_s + \eta_{bc} + \frac{1}{g\rho_0} p_b. \quad \text{(A.1)}$$

The terms on the right-hand side are due to upper ocean steric change, deep ocean steric change and change in bottom pressure.

According to Gill and Niiler (1973) the near surface steric anomaly

$$\eta_s = \frac{1}{\rho_0} \int_{-h}^{0} \rho'(z)\, dz \qquad (A.2)$$

is the dominant term on the large scales outside the tropics. Here $\eta'(z,t) = \rho(z,t) - \overline{\rho_0}(z)$ is the time-dependent density anomaly relative to a reference profile. The depth h represents the base of the seasonal thermocline taken to be 200 m by Gill and Niiler (1973). The upper ocean steric anomaly is made up of two terms

$$\eta_s = \frac{1}{\rho_0} \int_{-h}^{0} \frac{\partial \rho}{\partial T} T'\, dz + \frac{1}{\rho_0} \int_{-h}^{0} \frac{\partial \rho}{\partial S} S'\, dz. \qquad (A.3)$$

Estimates suggest that the second term can be neglected and that the steric height anomaly to the first order is determined by the change in the heat content of the seasonal thermocline (Gill and Niiler, 1973). Yan et al. (1995) demonstrated a near balance of the local heat storage rate on a spatial scale of 5° in the North Pacific. Accordingly, changes in the steric component are to the first order given by

$$\frac{\partial}{\partial t} \eta_s = \frac{1}{\rho_0} \int_{-h}^{0} \alpha(T,p) \frac{\partial}{\partial t} T'\, dz = \frac{\alpha Q'}{\rho_0 c_p}. \qquad (A.4)$$

where α is the thermal expansion coefficient, c_p is the specific heat of seawater and $T' = T - \bar{T}$ and $Q' = Q - \bar{Q}$ are the surface temperature and the heat flux anomalies, respectively.

It is clear from Eq. (A.4) that η_s entirely due to expansion and contraction of the water column but not due to changes in mass. Changes in η_s are, therefore, not associated with pressure gradients and currents below a shallow surface layer. Because of the large-scale nature of the steric anomalies, on the other hand, associated near-surface pressure gradients are generally small rendering steric height anomalies dynamically passive. Thus, the upper ocean steric height signal present in the satellite ssh data should be removed to reveal the dynamically active signals in the observations that are otherwise hidden.